



HAL
open science

DEM MODELLING OF DRY STONE RETAINING WALLS

Nathanaël Savalle, Eric Vincens, Fabian Dedecker

► **To cite this version:**

Nathanaël Savalle, Eric Vincens, Fabian Dedecker. DEM MODELLING OF DRY STONE RETAINING WALLS. Congresso de Métodos Numéricos em Engenharia, Jul 2019, Guimarães, Portugal. hal-04481937

HAL Id: hal-04481937

<https://hal.science/hal-04481937v1>

Submitted on 28 Feb 2024

HAL is a multi-disciplinary open access archive for the deposit and dissemination of scientific research documents, whether they are published or not. The documents may come from teaching and research institutions in France or abroad, or from public or private research centers.

L'archive ouverte pluridisciplinaire **HAL**, est destinée au dépôt et à la diffusion de documents scientifiques de niveau recherche, publiés ou non, émanant des établissements d'enseignement et de recherche français ou étrangers, des laboratoires publics ou privés.

See discussions, stats, and author profiles for this publication at: <https://www.researchgate.net/publication/334193772>

DEM MODELLING OF DRY STONE RETAINING WALLS

Conference Paper · July 2019

CITATIONS

0

READS

380

3 authors:



Nathanaël Savalle

Université Clermont Auvergne

25 PUBLICATIONS 119 CITATIONS

SEE PROFILE



Eric Vincens

Ecole Centrale de Lyon

71 PUBLICATIONS 924 CITATIONS

SEE PROFILE



Fabian Dedecker

ITASCA Consultants, S.A.S.

27 PUBLICATIONS 317 CITATIONS

SEE PROFILE

DEM MODELLING OF DRY STONE RETAINING WALLS

N. Savalle¹, E. Vincens¹ and F. Dedecker²

1: Ecole Centrale Lyon, University of Lyon
e-mail: nathanael.savalle,eric.vincens@ec-lyon.fr

2: ITASCA consultants S.A.S, Lyon
e-mail:f.dedecker@itasca.fr

Keywords: masonry, bricks, slope, highway, failure, heritage

Abstract *Dry stone retaining walls (DSRWs) are vernacular structures, which consist in a specific assemblage of individual rubble stones. Herein, we propose some recommendations to achieve a correct modelling of the mechanical behaviour of DSRWs towards failure with the use of the Discrete Element Method (DEM). There are two kinds of DSRWs, those that just retain slope and others that retain a road built on the top of the backfill.*

For walls retaining slopes, a full 2D DEM approach (PFC2D) was used as the most sophisticated way to study such a system and the modelling was validated on full scale experiments. The modelling retrieved in a very good way the features observed on site as the expense of much computation time. More interesting was the use of a mixed DEM-continuum approach (UDEEC) where the constitutive laws for the stone-stone contact and backfill-wall contact are averaged. Very efficient in terms of computation time, the process of identification of the model parameters is here much lighter than with a full DEM approach without losing precision for the prediction.

For walls retaining a slope with a highway a mixed 3D DEM-continuum approach (3DEC) was required. A straightforward methodology was proposed in order to correctly retrieve the features observed in both scaled down experiments or in full scale experiments.

In conclusion, the full DEM and the mixed DEM-continuum approaches were able to precisely capture the mechanical behaviour of DSRWs towards failure even if idealised blocks were used.

1 INTRODUCTION

There are many regions world wide that have been shaped by dry stone structures, due to the natural presence of required material: stones. More specifically, besides their cultural value, dry stone retaining walls (DSRWs) have always played some economic role: slope DSRWs help to shape and stabilize the landscape to enable agricultural activities while highways DSRWs enable the construction of transport facilities useful for any economic activity. At present, this heritage is very often fully damaged, generally

because DSRWs are very old and lacked some maintenance. However, very partial rules are available to design and repair such structures.

As these structures are built by assembling stones without any mortar bond, their resistance lies in friction mobilized between stones and in the careful assemblage that enables to maximize the wall density as well as a strong interlocking of stones. In spite of the absence of mortar, DSRWs can handle large deformations that can be linked to a deformable foundation soil, a weathering of the stones or a localised forces, like the one induced by vehicles on highways DSRWs [1, 2, 3].

Discrete (or Distinct) Element Methods are powerful tools to study the mechanical behaviour of DSRWs. Indeed, DEM tools allow the study of individual blocks in interaction in a simple way. In the past, DEM tools have been intensively used on many civil engineering systems, as they often display large or localized deformations. DEM tools have been developed in the late 1970s by Cundall and Strack [4]. At the beginning, it was designed to study granular materials with infinitely rigid grains (representing either powder [5], avalanche [6], sand grains [7] or steel balls [8]). Nowadays, several different methodologies have been developed to build DEM codes [4, 9, 10, 12]. Some of them can also handle deformable blocks [10, 11, 13].

In civil and geotechnical engineering, DEM methods have been used to study large systems, such as rockfill dams [14, 15], landslide [16, 17, 18], fractured rock masses [19, 20] and rock impact on structures [21, 22]. More specifically, DEM codes (and particularly a mixed DEM-FEM approach) have already been used to study the behaviour of dry stone retaining walls [1, 2, 3, 23, 24, 25].

This paper describes different DEM tools used to model the behaviour of DSRWs with the aim at being capable of designing new walls. First, slope retaining walls are studied with a full DEM approach followed by a mixed FEM-DEM approach. Then, highway retaining walls are studied using a mixed DEM-FEM approach. The paper presents some technical keys to ensure the obtention of results of high quality.

2 SLOPE RETAINING WALLS

2.1 Full DEM approach

A wall retaining slope is a geotechnical work composed of three sub-systems: the wall, the backfill and the backfill-wall interface (Figure 1). An attempt was made to model the full-scale experiments carried out by Colas *et al.* [26] where the backfill was composed of a purely frictional material. Due to the mode of failure of such walls, ITASCA code *PFC2D* (Particle Flow Code) was used [4]. In this code, the basic elements are rigid disks but more complex bodies can be created by bonding several disks together. The new object that results from this merging is handled as a rigid or a deformable single body [27]. At each time-step, the calculation runs in alternate between contact-force laws and laws of motion. The particularity of DEM codes is related to the existence of a contact law between the interacting bodies. The simplest contact law (linear contact law) that can be chosen consists of a spring, where the magnitude of the normal force

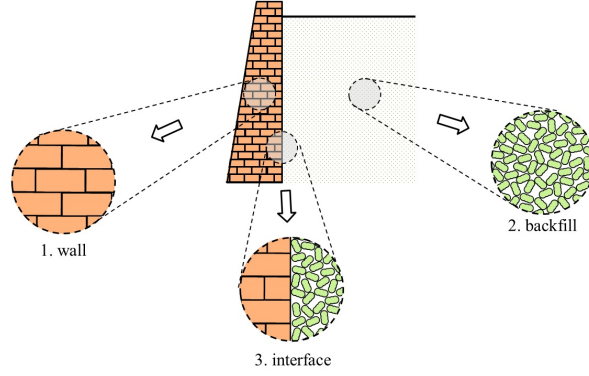


Figure 1: Three sub-systems for DSRWs.

F_n and of the incremental tangential force ΔF_t is calculated as follows:

$$F_n = k_n \Delta U_n \quad (1)$$

where U_n is the normal relative displacement between the two bodies in interaction and k_n the normal stiffness of the contact.

$$\Delta F_t = -k_t \Delta U_t \quad (2)$$

where ΔU_t is the incremental tangential relative displacement between the two bodies in interaction and k_t the tangential stiffness of the contact. Sliding may occurs at contact when:

$$F_t = F_n \tan \psi \quad (3)$$

where ψ is the contact friction angle.

Blocks were recreated using a given number of disks poured in a box and were bonded together to form a new rigid body with deformable contacts. The inner disks of the block were erased keeping the disks giving the outer shape of the blocks (Figure 2). These blocks present some geometrical roughness that was supposed to be representative of actual blocks.

Accordingly, the backfill grains were recreating by bonding three particles together.

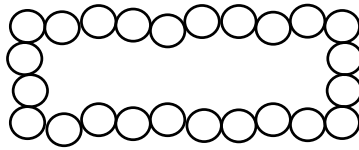


Figure 2: Block model for the wall.

The shape was calibrated in such a way that the internal friction angle of the actual granular material can be retrieved.

The last sub-system which is the backfill-wall interface naturally arises from the contact between the backfill grains and the disks forming the outer shape of the blocks. Specific properties were affected to this interface.

If a linear contact law was used for the contact between the backfill grains and between these latter and the wall blocks, another constitutive law was used for the block-block contact due to a problem of transmission of information between interacting blocks. A so-called smooth-joint contact law [30] which basically removes the block geometrical roughness was chosen. This contact law resembles the linear contact law except that: (1) the contact plane direction is the same and imposed at each disk contact and (2) sliding occurs along a given contact area A (or length in 2D model) (Figure 3). Then, this contact law is similar to a homogenized contact law and the macro roughness was not taken into account between block-block contacts.

The mechanical parameters for the different types of contact were identified by sim-

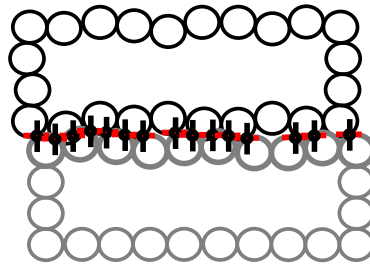


Figure 3: Smooth-joint contact law between wall blocks.

ulating experiments representative of the different sub-systems [29]: a biaxial test for the backfill grains [29], a Constant Normal Load direct shear test for the backfill wall interface [29] (Figure 4). Much effort was required for the identification of the parameters involved in the backfill. First, the actual critical state angle of 32° was retrieved by a trial-and-error method which led to the determination of the contact friction angle. Then, the backfill porosity was identified in order to obtain an internal friction angle of 37.7° . A trial-and-error was also used to identify the contact friction angle for the backfill wall interface. Finally, in the case of the block-block contacts, the microscopic parameters are equal to parameters existing at the global scale since a homogenized contact law was used.

In Figure 5, the loading process of the wall by the backfill is shown together with the

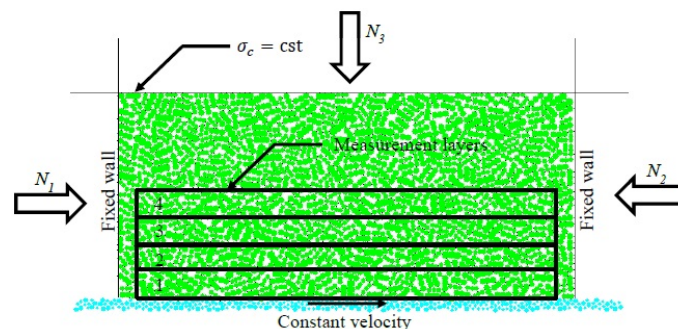


Figure 4: Model for the CNL direct shear test for the backfill wall interface.

typical mode of failure when the critical backfill height was reached. Three full scale

experiments involving different materials for the wall stones (lime and schist) were simulated and a maximum relative error of 7% with respect to actual experiments for the critical backfill height leading to failure was found. However, 2.5 weeks of computation (Intel Xeon CPU 3.2 GHz) were required for processing the creation of the 2.5m high backfill, layer by layer, until reaching the critical backfill height.

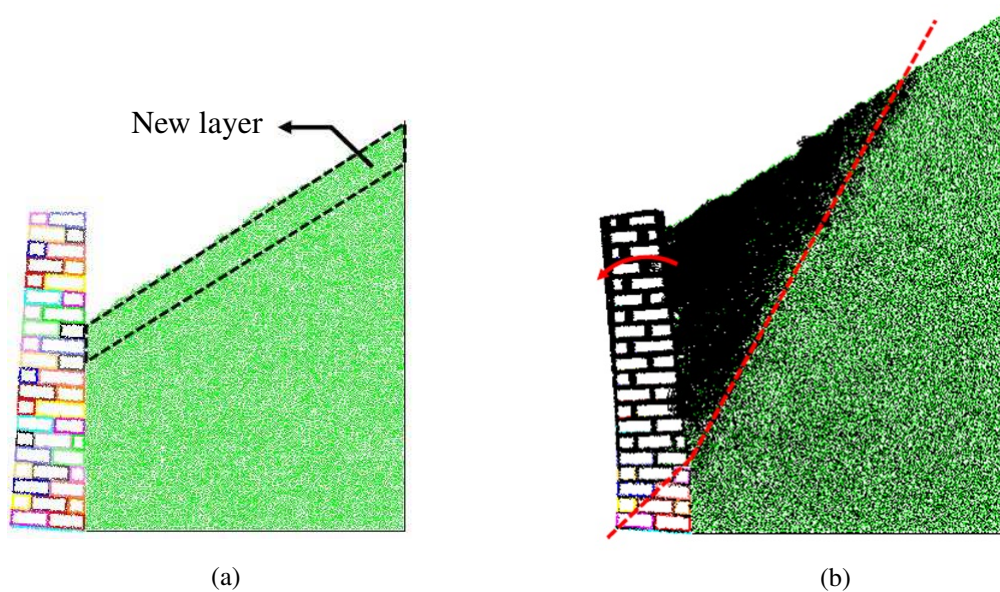


Figure 5: Loading of the DSRW by the backfill: (a) Creation of a layer and (b) system at failure, velocity field.

2.2 Mixed DEM-continuum approach

Due to the drawbacks of the fully DEM approach which requires high computation time, involves a heavy process for the creation of the individual objects (creation of shapes and heterogeneities) and for the identification of the local parameters, another approach was used to solve the problem of the stability of slope DSRWs. In particular, ITASCA code *UDEC* (Universal Distinct Element Code) was used to model the loading of the DSRWs with a backfill.

The wall was kept as a set of individual bodies while the backfill was modeled as a continuum system. The wall is created by defining its outer shape and the blocks were eventually generated by the use of cutting planes. The blocks were considered as deformable bodies following a Hooke law and the contact between blocks was also taken as deformable requiring the definition of a normal and a tangential stiffness. The contact supposing to develop friction, a homogenized Coulomb law was used which required the calibration of a frictional coefficient.

The whole backfill meshing was built from the very beginning but the elements were activated gradually from bottom to top to mimic the actual process of the wall loading that was used in the full scale experiments (Figure 6(a)). A non-associated elastic per-

factly plastic Mohr-Coulomb model was chosen for the backfill. For details about all the numerical parameters, see Oetomo [28].

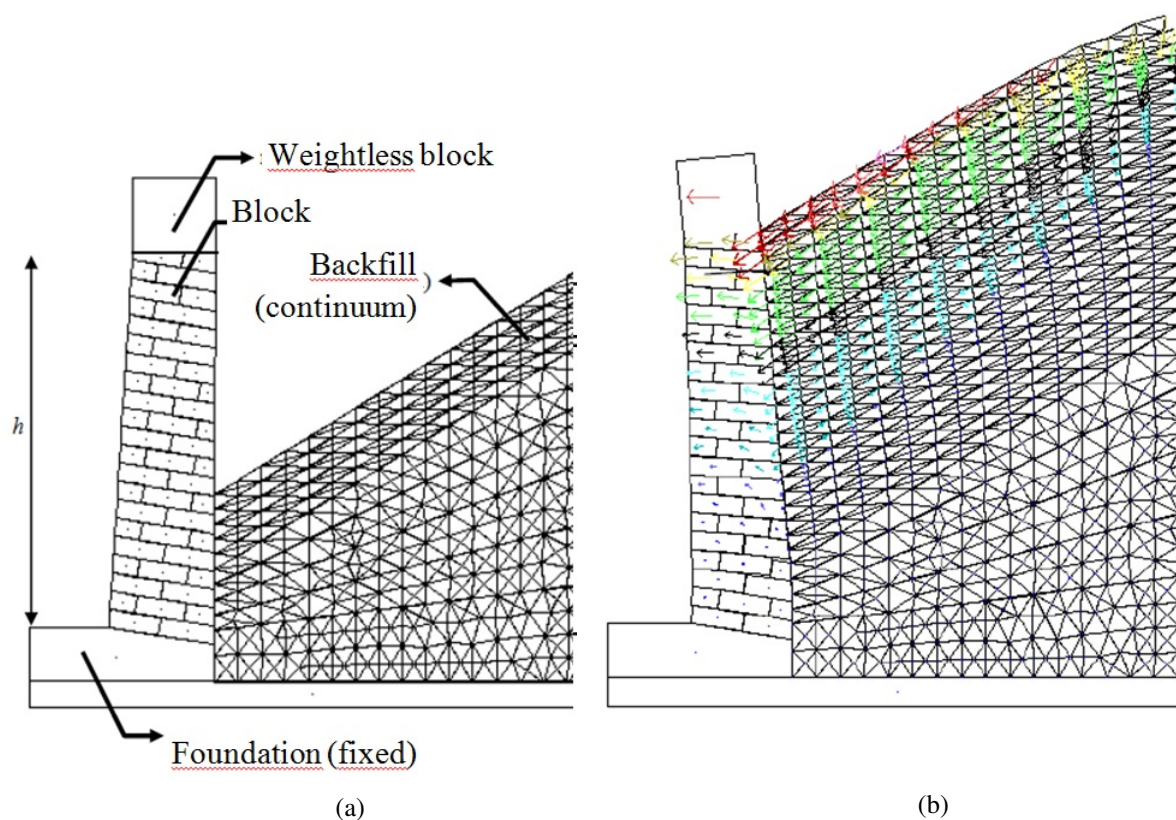


Figure 6: Mixed DEM-continuum modelling of a DSRW: (a) Construction of the backfill and (b) System at failure, velocity field.

The backfill-wall interface mechanical behaviour was ruled by an homogenized constitutive law (elastic perfectly plastic) for which an internal friction angle and a cohesion have been identified.

In this case, the identification of the model parameters was facilitated since the constitutive laws for the backfill and for the backfill-wall interface were defined at the scale of the Representative Elementary Volume. A typical result at failure is given in Figure 6(b). We found a maximum relative error of 7% for the critical backfill height leading to failure which is similar to what was obtained for the fully DEM approach while the computation time was reduced to 4h on the same type of computer (Intel Xeon CPU 3.2 GHz).

2.3 Pseudo-static tests

To complete the static study of dry stone retaining walls (DSRWs), a seismic study of slope DSRWs has been carried out. It consisted in an experimental campaign on a scaled-down mock-up of a slope DSRW. A wall made of parallelepiped clay bricks

retaining a sandy backfill was progressively tilted until failure [31]. This pseudo-static experiment is to be bridged with the actual recommendation of the Eurocode 8. Based on this experimental campaign, a numerical model has been developed to retrieve the tests results [32]. All the ten experimental retaining brick walls (each having a different aspect ratio height H over base B) were simulated.

As *UDEC* has proven relevant to model DSRWs, this mixed DEM-continuum code has been chosen for the modelling of the pseudo-static tests. Following the same procedure as Oetomo [28], the wall was made of individual bricks whereas the backfill was modelled as a single deformable block, with a Mohr-Coulomb elastic plastic constitutive law. Similarly, joints between bricks followed a Mohr-Coulomb elastic plastic law (with zero cohesion). Once the model was defined and its stability checked, the natural gravity was progressively inclined which is in fact equivalent to the experimental procedure that consisted in tilting the whole mock-up (backfill, wall and container). For each increase of the gravity inclination (0.1°), the kinetic energy of the wall through block velocities and masses was computed. After defining relevant thresholds, the wall was considered stable if its energy was below a first threshold during five consecutive steps (a step = 300 computational cycles). On the contrary, it was considered at failure when its energy was above a second threshold 200 times (not necessarily consecutive). The resulting tilting angle of the gravity at failure of the wall was compared to the experimental one.

Contrary to the modelling of the full-scale experiments, involving stone blocks of different sizes (from 1cm to 50cm), the bricks used in the experiments were fully parallelepipedic. The assemblage used to build the wall was periodic (Figure 7). Since it mixes headers and stretchers (as done in practice by drystone masons), choosing the representative cross-section to be used in the numerical simulations with a plane strain code (*UDEC*) was not an easy task. To overcome this problem, all the possible cross-sections were studied separately, and a weighting coefficient for each configuration was computed, based on the occurrence of each cross-section in the wall. For the experimental studied walls, four different cross-sections were identified (Figure 8). More details about the numerical procedure and parameters can be found in [32].

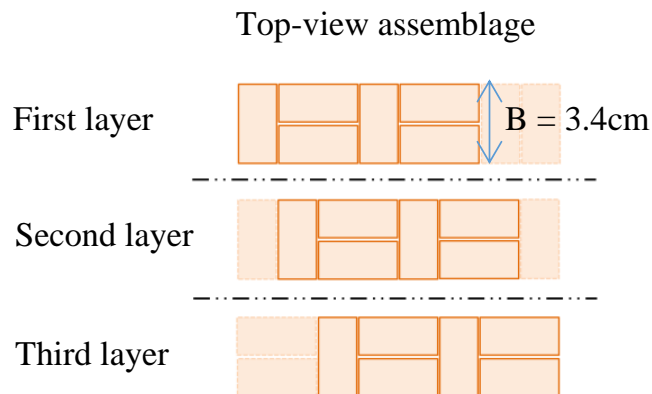


Figure 7: Assemblage used to build the brick walls. A mix of headers and stretchers is used.

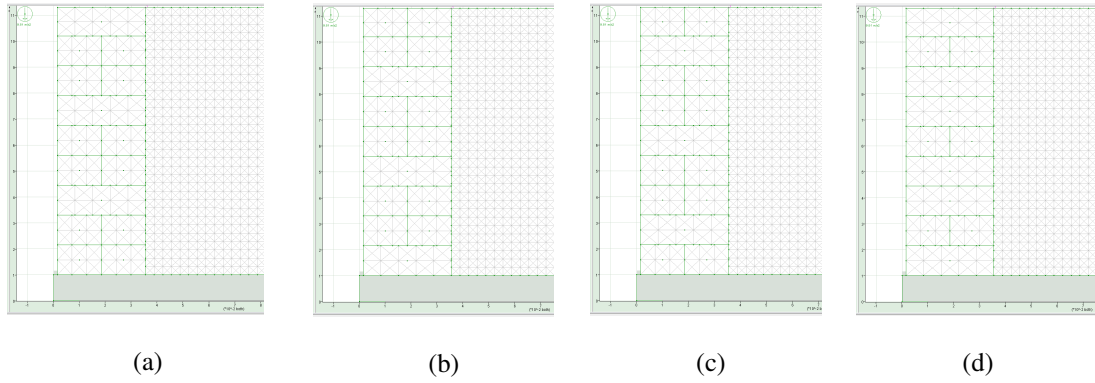


Figure 8: The four different cross-sections identified in the experiments.

Comparing the numerical results to the experimental ones, the numerical simulation proved to be relevant to catch the driving phenomena. Not only the numerical (predicted) tilting angles at failure of the wall were in agreement with the experimental ones (maximum departure of 13%; mean departure of 8%), but also the two modes of failure (sliding and toppling) were numerically retrieved. The more slender walls fell with a toppling mode (Figure 9a) while less slender walls fell according to a sliding mode (Figure 9b). Moreover, the transition between the two modes of failure has been found around the slenderness (or aspect ratio) $H/B = 2.0$ in the numerical simulations which is in accordance with the experimental transition obtained for $H/B = 1.9$.

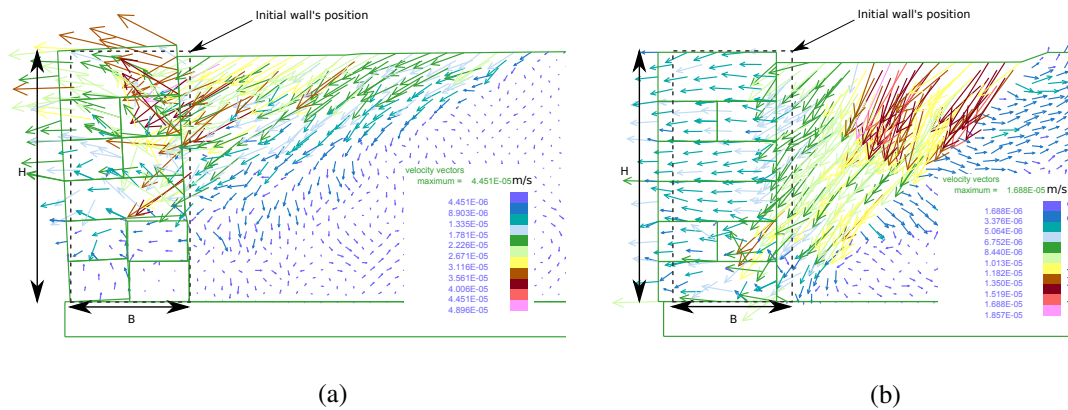


Figure 9: Brick wall at failure. (a) Toppling mode of failure. (b) Sliding mode of failure.

3 HIGHWAY RETAINING WALLS

Highway DSRWs are works for which a concentrated loading is applied at the backfill surface which complements the direct backfill pressure on the retaining wall. This concentrated loading models the weight of vehicles (transferred by the contact between the

wheels and the road surface) operating on the road.

Scaled-down experiments were simulated with *3DEC* (ITASCA code) since a true three-dimensional mode of failure was found in the experiments. This code allows the equilibrium of deformable polyhedral bodies in interaction to be computed. In this respect, it is similar to *UDEC* but this latter code can only handle plane strain systems. In the experiments, steel blocks were superposed one on each other at a given distance d from the inward backfill wall to model the concentrated load. Three distances were tested in the experiments: 2cm, 3cm and 4cm and the critical concentrated load leading to failure was investigated. Clay bricks were used to build the wall with an assemblage compatible with the one use in actual dry stone retaining walls and sand was used to load the wall.

In the numerical simulation, the wall was created from a single block that was split by different cutting planes in order to generate parallelepiped blocks. The backfill was created in a single stage and the meshing size of the backfill was reduced within the zone where the concentrated loading was placed (Figure 10). The reduction of the meshing size allows eight grid-points of the backfill to be involved in the transfer of forces to each wall bricks within the wall-backfill interface. More details can be found in [33].

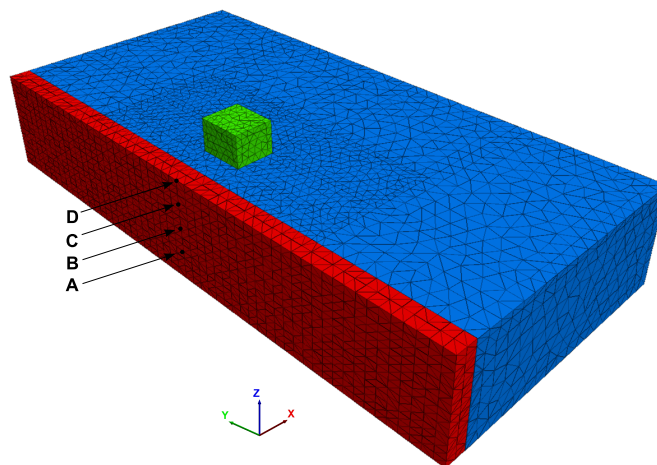


Figure 10: Numerical model for the wall loading by a concentrated loading; points A, B, C, D are measurement points.

The wall bricks were supposed to be deformable following a Hooke law and the joint between the wall bricks was ruled by a Coulomb-slip model where the incremental law for both the normal force and the tangential force were linear. The behavior of the backfill was modelled by an elastic perfectly plastic Mohr-Coulomb constitutive law and the joint between the wall and the backfill was handled the same way as a joint between blocks.

Some preliminary calculations revealed that the perfect contacts between the wall bricks tended to generate jammed states which induced the absence of a clear steady state when increasing the concentrated loading [33]. This latter feature is not consistent with the

observations throughout the down-scale experiments. In fact, the perfect contact planes may not exist in the down-scale experiments due to the imperfections of the clay bricks. Simulations have proven that a gap of 0.5mm (5% of brick thickness) between the vertical contact planes was able to remove this bias. Above this threshold value, the result became independent of the gap value.

The results for the vertical concentrated force on the backfill surface leading to failure throughout the simulations were compared to the results obtained throughout the experiments (Figure 11). The simulations led to results corresponding to the average value obtained throughout the experiments except for the smaller distance d of 2cm. In this latter case, a departure of 8% with the experimental average value was found which is still acceptable. It came from the loss of contact between the backfill and the wall where the backfill meshing followed the punching of the backfill by the block. This bias could not be mitigated and is inherent to the limits of the continuum approach.

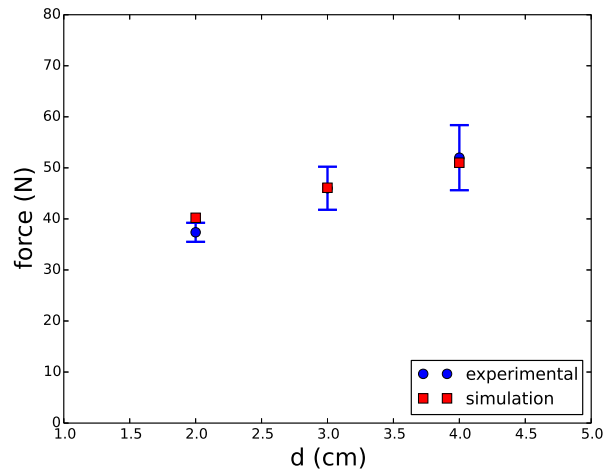


Figure 11: Maximum vertical force on the backfill surface inducing the total wall failure for different distances d of the steel blocks to the inward wall face. the.

4 CONCLUSION

This paper summarizes different studies related to the mechanical behaviour of dry stone retaining walls under static conditions. Due to the discrete nature of the wall, a DEM approach seemed an appropriate technique for addressing this boundary value problem. A fully 2D DEM approach where the backfill was modeled as a set of elongated particles, though precise, put into light some drawbacks inherent to the approach such as the heavy process for the identification of the local parameters and a high computation time. Additionally, there are drawbacks due to the 2D modeling such as the existence of local heterogeneities in the backfill and in the backfill–wall interface that does not allow a correct transmission of information.

A mixed plain strain DEM-continuum approach where the backfill was modeled by a continuum deformable medium has been found much more efficient in terms of compu-

tation time and easiness to define the model parameters and provided accurate results. Some limits arose at the time when walls with different sets of periodic assemblages were studied and the choice of the wall representative section in a plain strain approach was to be made.

A highway DSRW was modeled with a mixed 3D DEM-continuum approach that required to involve some gap between the vertical joints of stones to avoid unrealistic jammed states. Very accurate results were obtained except in the case when the concentrated load was close to the wall since it led to some detachment of the backfill meshes from the retaining walls. It tended to overestimate the resistance of the retaining wall but the estimate was considered as in a fairly good agreement with the experiments.

In general, the prediction of the resistance of the DSRW was very good and in few cases only fairly good with respect to experimental results for either slope DSRWs with static or pseudo-static conditions or for highway DSRWs with static conditions. We recommend the use of the DEM-continuum approach to address the case of masonry retaining walls.

REFERENCES

- [1] W. Powrie, R.M. Harkness, X. Zhang and D.I. Bush, "Deformation and failure modes of drystone retaining walls", *Géotechnique*, Vol. **52 no.6**, pp. 435-446, (2002).
- [2] M. Claxton, R.A. Hart, P.F. McCombie and P.J. Walker, "Rigid block distinct-element modelling of dry-stone retaining walls in plane strain", *ASCE Journal of Geotechnical and Geoenvironmental Engineering*, Vol. **131 no.3**, pp. 381-389, (2005).
- [3] P. Walker, P.F. McCombie and M. Claxton, "Plane strain numerical model for dry-stone retaining walls", *Proceedings of the Institution of Civil Engineers - Geotechnical Engineering*, Vol. **160 no.2**, pp. 97-103, (2007).
- [4] P.A. Cundall and O.D.L. Strack, "A discrete numerical model for granular assemblies", *Géotechnique*, Vol. **29 no.1**, pp. 47-65, (1979).
- [5] S. Shima, H. Kotera and Y. Ujie, "A Study Of Constitutive Behaviour Of Powder Assembly By Particulate Modeling", *Journal of the Society of Materials Science, Japan*, Vol. **44**, pp. 163-168, (1995).
- [6] D. Salciarini, C. Tamagnini and P. Conversini, "Discrete element modeling of debris-avalanche impact on earthfill barriers", *Physics and Chemistry of the Earth*, Vol. **35 no.3-5**, pp. 172-181, (2010).
- [7] C. Noguier-Lehon, B. Cambou and E. Vincens, "Influence of particle shape and angularity on the behaviour of granular materials: a numerical analysis", *International Journal for Numerical and Analytical Methods in Geomechanics*, Vol. **27 no.14**, pp. 1207-1226, (2003).

- [8] C. Nouguié-Lehon, M. Zarwel, C. Diviani, D. Hertz, H. Zahouani and T. Hoc, “Surface impact analysis in shot peening process”, *Wear*, Vol. 302 no.1-2, pp. 1058-1063, (2013).
- [9] B.J. Alder and T.E.W.A. Wright, “Studies in molecular dynamics. II. Behavior of a small number of elastic spheres”, *The Journal of Chemical Physics*, Vol. **33 no.5**, pp. 1439-1451, (1960).
- [10] G.G.W. Mustoe, “A Generalized formulation of the discrete element method”, *Engineering Computations*, Vol. **9 no.2**, pp. 181-190, (1992).
- [11] G.-H. Shi, “Discontinuous deformation analysis: A new numerical model for the statics and dynamics of deformable block structures”, *Engineering Computations*, Vol. **9 no.2**, pp. 157-168, (1992).
- [12] J.R. Williams, “Contact analysis of large numbers of interacting bodies using discrete modal methods for simulating material failure on the microscopic scale”, *Engineering Computations*, Vol. **5 no.3**, pp. 198-209, (1988).
- [13] J. Ghaboussi, “Fully deformable discrete element analysis using a finite element approach”, *Computers and Geotechnics*, Vol. **5 no.3**, pp. 175-195, (1988).
- [14] R. Deluzarche and B. Cambou, “Discrete numerical modelling of rockfill dams”, *International Journal for Numerical and Analytical Methods in Geomechanics*, Vol. **30 no.11**, pp. 1075-1096, (2006).
- [15] C. Silvani, T. Desoyer and S. Bonelli, “Discrete modelling of time-dependent rock-fill behaviour”, *International Journal for Numerical and Analytical Methods in Geomechanics*, Vol. **33 no.5**, pp. 665-685, (2009).
- [16] L.J. Lorig, A.D. Watson, C.D. Martin and P.D. Moore, “Rockslide run-out prediction from distinct element analysis”, *Geomechanics and Geoengineering: An International Journal*, Vol. **4 no.1**, pp. 17-25, (2009).
- [17] G. Mollon and J. Zhao, “Fourier–Voronoi-based generation of realistic samples for discrete modelling of granular materials”, *Granular Matter*, Vol. **14 no.5**, pp. 621-638, (2012).
- [18] V. Bonilla-Sierra, L. Scholtes, F.V. Donze and M.K. Elmouttie, “Rock slope stability analysis using photogrammetric data and DFN–DEM modelling”, *Acta Geotechnica*, Vol. **10 no.4**, pp. 497-511, (2015).
- [19] P. Moarefvand and T. Verdel, “The probabilistic distinct element method”, *International Journal for Numerical and Analytical Methods in Geomechanics*, Vol. **32 no.5**, pp. 559-577, (2007).

- [20] M.N. Bidgoli and L. Jing, “Anisotropy of strength and deformability of fractured rocks”, *Journal of Rock Mechanics and Geotechnical Engineering*, Vol. **6 no.2**, pp. 156-164, (2014).
- [21] F. Nicot, P. Gotteland, D. Bertrand and S. Lambert, “Multiscale approach to geocomposite cellular structures subjected to rock impacts”, *International journal for numerical and analytical methods in geomechanics*, Vol. **31 no.13**, pp. 1477-1515, (2007).
- [22] C. Salot, P. Gotteland and P. Villard, “Influence of relative density on granular materials behavior: DEM simulations of triaxial tests”, *Granular Matter*, Vol. **11 no.4**, pp. 221-236, (2009).
- [23] P.J. Walker and J.G. Dickens, “Stability of medieval dry stone walls in Zimbabwe”, *Géotechnique*, Vol. **45 no.1**, pp. 141-147, (1995).
- [24] J.G. Dickens and P.J. Walker, “Use of distinct element model to simulate behaviour of dry-stone walls”, *Structural Engineering Review*, Vol. **2-3 no.8**, pp. 187-199, (1996).
- [25] R.M. Harkness, W. Powrie, X. Zhang, K.C. Brady and M.P. O’Reilly, “Numerical modelling of full-scale tests on drystone masonry retaining walls”, *Géotechnique*, Vol. **50 no.2**, pp. 165-179, (2000).
- [26] A.-S. Colas, J.-C. Morel and D. Garnier, “Full-scale field trials to assess dry-stone retaining wall stability”, *Engineering Structures*, Vol. **32 no.5**, pp. 1215-1222, (2010).
- [27] Itasca Consulting Group INC. *Particle Flow Code in 2 Dimensions: Theory and Background*, Itasca: Minnesota, Fourth Edition, (2008).
- [28] J.J. Oetomo, “Comportement à la rupture des murs de soutènement en pierre sèche : une modélisation discrète (in French)”, *PhD thesis, Ecole centrale de Lyon*, (2014).
- [29] J.J. Oetomo, E. Vincens, F. Dedecker and J.-C. Morel, “Modeling the 2D behavior of drystone retaining walls by a fully discrete element method”, *International Journal for Numerical and Analytical Methods in Geomechanics*, Vol. **40 no.7**, pp. 1099-1120, (2016).
- [30] D.M. Ivars, D. Potyondy, M. Pierce and P.A. Cundall, “The smooth-joint contact model”. *8th World Congress on Computational Mechanics and 5th European Congress on Computational Methods in Applied Sciences and Engineering, 2008, WCCM ECCOMAS, Venezia* (2008), Paper No. a2735.
- [31] N. Savalle, E. Vincens, S. Hans, “Pseudo-static scaled-down experiments on dry stone retaining walls: Preliminary implications for the seismic design”, *Engineering Structures*, Vol. **171**, pp. 336-347, (2018).

- [32] N. Savalle, E. Vincens, S. Hans, “Experimental and numerical studies on scaled-down dry-joint retaining walls:Pseudo-static approach to quantify the resistance of a dry-joint brick retaining wall”, *Bulletin of Earthquake Engineering*, DOI 10.1007/s10518-019-00670-9 (2019).
- [33] J.-C. Quezada, E. Vincens, R. Mouterde and J.-C. Morel, “3D failure of a scale down dry stone retaining wall: a DEM modeling”, *Engineering Structures*, Vol. **117**, pp. 506-517, (2016).
- [34] O.C. Zienkiewicz and R.L. Taylor, *The finite element method*, McGraw Hill, Vol. I, 1989, Vol. II, (1991).
- [35] J.C. Simo and R.L. Taylor, “Consistent tangent operators for rate-independent elastoplasticity”, *Comput. Methods Appl. Mech. Eng.*, Vol. **48**, pp. 101-118, (1985).
- [36] F. Armero and S. Glaser, *Enhanced strain finite element methods for finite deformation problems*. M. Doblaré, J.M. Correas, E. Alarcón, L. Gavete and M. Pastor eds. *III Congreso de Métodos Numéricos en Ingeniería, Zaragoza, 1996*, SEMNI, Barcelona (1996), pp. 423-437.